Crystallization Behaviors and Mechanical Performance of Polypropylene/Tetrapod-Shaped Zinc Oxide Whisker Composites

Wen Bianying, Ji Binbin

Department of Material Science and Engineering, School of material and mechanical engineering, Beijing Technology and Business University, Beijing 100048, People's Republic of China

ABSTRACT: Polypropylene (PP)/tetrapod-shaped zinc oxide whisker (T-ZnOw) composites are prepared via a melt-mixing method in combination with a Haake rheometer. Differential scanning calorimetery (DSC) is used to investigate the nonisothermal and isothermal crystallization behaviors of the composites. Crystalline morphology is observed using hot-stage optical microscopy, and the mechanical performance of the composites is investigated. Results indicate that T-ZnOw has no heterogeneous nucleation effect on PP; in fact, it retards the growth of the crystal. Filled T-ZnOw in PP matrix decreases the peak crystallization and melting temperatures of PP. T-ZnOw shows either a reinforcing or toughening effect on the PP matrix at very lower weight ratios. These effects, however, decline with increasing T-ZnOw contents because the size of the spherulitic crystals becomes bigger. © 2011 Wiley Periodicals, Inc. J Appl Polym Sci 124: 138–144, 2012

Key words: tetrapod-shaped zinc oxide whiskers; polypropylene; crystallization behavior; morphology; mechanical performance

INTRODUCTION

Inorganic whiskers have recently attracted more attention in the field of polymer modification.[1–3] Among the whiskers available, tetrapod-shaped zinc oxide whiskers (T-ZnOw) have gained importance because of their unique structures and good comprehensive properties, which include semiconductivity, wear resistance, vibration insulation, and microwave absorption.[4–8] In contrast to common whiskers, T-ZnOw has a perfect 3D structure, which avoids oriented distribution and endows the polymeric composites with isotropic, rather than anisotropic properties.[9] Even so, it does not get wide variety of applications in functional material area because the mechanism in which T-ZnOw affects a polymer matrix is not very clear.

It is recognized that some inorganic fillers, such as potassium-titanate whiskers, clay, talc, calcium carbonate, etc., can usually induce nucleation for matrix crystallization[10] and accelerate the overall crystallization process. In this work, we use polypropylene (PP, a typical semicrystalline polymer with excellent processing performance) as a matrix to investigate the role of T-ZnOw in polymer composites and determine whether T-ZnOw can induce heterogeneous nucleation for crystallization of the matrix and still exhibit toughening and strengthening effects on PP matrix.

EXPERIMENT

Materials and specimen preparation

PP (K1008), with a melt flow rate of 10 g/10 min (230°C, 2160 g), was purchased from the Beijing Yanshan branch of China Petroleum and Chemical Co., Ltd.; T-ZnOw (AT01) was purchased from Chengdu Crystrealm Co., Ltd., China. The weight shares for PP were fixed at 100, while those for T-ZnOw were 1, 3, and 5, respectively. To avoid influences from other factors, T-ZnOw was not treated with any coupling agent.
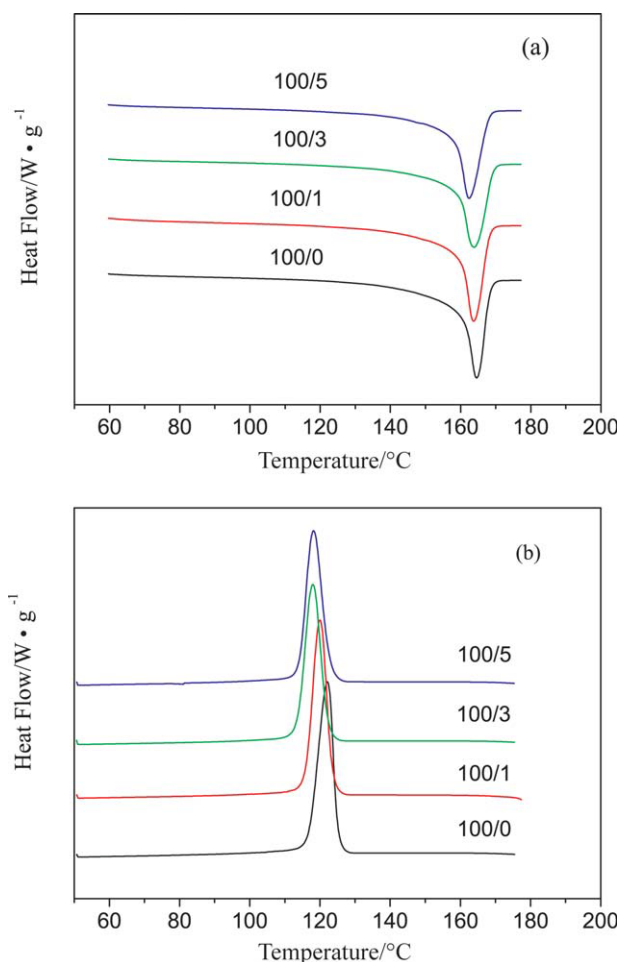
PP and T-ZnOw were mixed and melted using a Haake rheometer (Haake Polylab OS RheoDrive4) at 200°C and 35 rpm for 8 min. The composite was then reheated and pressed using a plate presser (Lab Tech Engineering Co., Ltd., Sweden) at 200°C and 5 MPa for 5 min, and then cooled to ambient temperature. Finally, the flat material was incised to normal specimens for testing.

Figure 1 DSC thermograms of PP/T-ZnOw composites in non-isothermal crystallization: (a) Melting curves; (b) cooling curves. [Color figure can be viewed in the online issue, which is available at wileyonlinelibrary.com.]

Differential scanning calorimetry procedures

Nonisothermal and isothermal crystallizations were carried out using a differential scanning calorimeter (DSC) type Q100 (TA Instruments). All DSC measurements were performed under a nitrogen atmosphere at a constant flow rate. Each sample was used only once to avoid any effects that may result from thermal degradation after the high temperature treatments. Sample weights were between 4 and 5 mg. During nonisothermal crystallization, samples were quickly heated to 180°C and kept for 5 min at this temperature to eliminate any previous thermal history. Then, they were cooled to 50°C with a cooling rate of 10°C/min and to obtain the crystallization curves; and then, were heated to 180°C again with a heating rate of 10 °C/min to obtain the melting curves. During isothermal crystallization, samples also were quickly heated to 180°C and kept for 5 min at this temperature to eliminate any previous thermal history. They were then cooled with a cooling rate of 30 °C/min to predetermined crystalliza-

tion temperatures (T_c) and maintained at that T_c to get an isothermal crystallization curve. The isothermal crystallization temperatures ranged from 124 to 130°C, in steps of 2°C.

Hot-stage optical microscopy observation

An Olympus BX51 polarizing optical microscopy (POM) equipped with a Linksys 32 DV hot stage thermal controller was used to investigate the spherulitic morphology of PP/T-ZnOw composites. Sample was pressed between two glass slides and was heated to 200°C for 3 min to erase any thermal history, cooled to 145°C at a rate of 10 °C/min, and then further cooled to 120°C at a rate of 1 °C/min. The crystallization procedure was observed and morphologies were recorded by photographs taken at several characteristic temperatures.

Mechanical performance test

Tensile strength was determined using a Zwick/Roell Z050 tester at a tensile rate of 2 mm/min according to GB/T1040-1992. Impact strength tests were run using a combined digital impact tester XJZ-50 according to GB/T1843-1996. The average value of tensile strength and impact strength of each sample was obtained from five tests.

RESULTS AND DISCUSSION

Nonisothermal crystallization behavior analyses

The effects of T-ZnOw on the nonisothermal crystallization behavior of PP were analyzed through DSC experiments. Figure 1 shows the crystallization thermograms of PP and PP/T-ZnOw composites at heating or cooling rates of 10 °C/min. From these plots, the peak crystallization temperature (T_c) and peak melting temperature (T_m) were obtained. The fusion enthalpy (ΔH_m), which evolved during crystal melting, was recorded as well. The results are summarized in Table I.

Only one peak was observed from the DSC curves presented in Figure 1(a,b). This means that all samples had only one crystalline form, i.e., the α-form. As shown in Table I, both T_c and T_m decrease with increasing T-ZnOw content. For example, the T_c and T_m

TABLE I
DSC Data of PP/T-ZnOw Composites During Non-Isothermal Crystallization

PP/T-ZnOw	T_c (°C)	T_m (°C)	ΔH_m (J g^{-1})	X_c (%)
100/0	122.1	164.6	91.18	43.6
100/1	120.0	163.8	91.85	44.4
100/3	118.0	163.8	89.35	44.0
100/5	118.1	162.4	87.09	43.8

of PP/T-ZnOw at the weight ratio of 100/5 were 118.1°C and 162.4°C, respectively. These are about 4°C and 2.2°C less than those of pure PP. These results are remarkably different from findings on other inorganic filled systems, such as potassium-titanate whiskers, talc, etc, and filled PP system.[11–13] In these systems, both the T_c and T_m increased when filled with inorganic fillers.

The main difference on property between T-ZnOw and other inert inorganic fillers are: on one hand, T-ZnOw is a semiconductor, it has conductive ability, which allows PP molecular chains to move better at lower crystallization temperatures; on the other hand, it has 3D structure, which is too complicated to induce PP molecular chains to assemble around it and this makes the final crystal maybe have a little loose in structure. So the decrease of both crystal melting temperature and crystallization temperature may be caused by these two reasons.

The relative degree of crystallinity (X'_c) is calculated from eq. (1) as:

$$X'_c = \frac{\Delta H_m}{\Delta H_m^0 (1 - \phi)} \tag{1}$$

here, ΔH_m is the fusion enthalpy of the samples, ΔH_m^0 is the fusion enthalpy of PP at absolute crystallization, $\Delta H_m^0 = 209$ J/g,[14] and ϕ is the weight fraction of the filler in the composite. The last column in Table I shows that the crystallinity changes minimally with filled T-ZnOw in PP. The reason for that refers to the isothermal crystallization procedure.

Isothermal crystallization behavior analyses

To describe the isothermal crystallization of PP/T-ZnOw samples, the Avrami equation[15] was employed. According to the classical equation:

$$X_c = 1 - \exp(-Kt^n) \tag{2}$$

where X_c is the relative crystallinity, corresponding to the crystallization time t, K is the Avrami crystallization rate constant, containing both the primary nucleation rate and the crystal growing rate, and n is the Avrami exponent, which depends on the mechanism of nucleation and on the form of crystal growth. Traditionally, for the convenience of graphic representation, eq. (2) is changed by a mathematical transformation to:

$$\log[-\ln(1 - X_c)] = n\log t + \log K \tag{3}$$

From the plot of $\log[-\ln(1 - X_c)$ versus $\log t$, n (slope of the straight line) and K (intersection with the y-axis) can be obtained. In addition, the maximum heat flow time can also be obtained by two derivations of eq. (2):
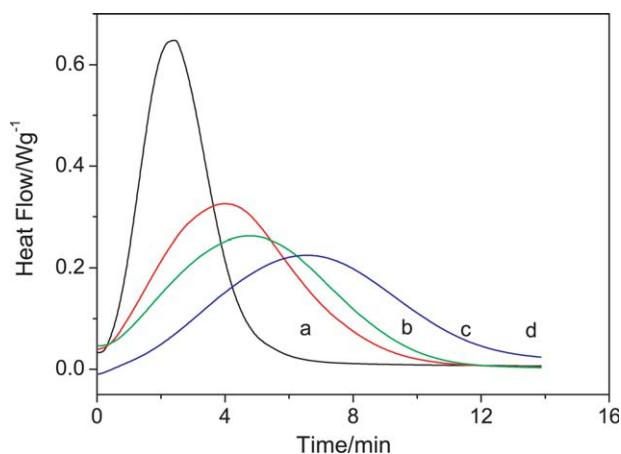
Figure 2 Isothermal crystallization curves of PP/T-ZnOw composites at 130 °C: (a) 100/0; (b) 100/1; (c) 100/3; (d)100/5. [Color figure can be viewed in the online issue, which is available at wileyonlinelibrary.com.]

$$t_{\max} = [(n - 1)/nK]^{1/n} \tag{4}$$

The crystallization half-time, $t_{1/2}$, is defined as the time at which the extent of crystallization is 50%, and is regarded as a very important crystallization kinetic parameter. If $X_c = 0.5$, the relationship between $t_{1/2}$ and K can be described as in eq. (5):

$$t_{1/2} = (\ln 2/K)^{1/n} \tag{5}$$

Furthermore, the crystallization rate $G_{1/2}$ is derived from $t_{1/2}$, according to eq. (6):

$$G_{1/2} = 1/t_{1/2} \tag{6}$$

The following discussions analyze the experimental data based on the Avrami approach.

Effect of T-ZnOw content on isothermal crystallization behaviors

Figure 2 illustrates a typical DSC crystallization exotherm for the isothermal crystallization of PP/T-ZnOw at T_c 130°C after complete melting at 180°C for 5 min. The exotherm peak became wider and weaker with increasing T-ZnOw content, while the maximum heat flow time $t_{\max}$ became longer. The results indicate that the introduction of T-ZnOw does not accelerate the crystallization rate of PP. The variation in relative crystallinity (X_c) is related to the generated heat ratio at time t.

At any given time, X_c is defined in the following equation as:

$$X_c = X(t)/X(\infty) = \int_0^t \frac{dH(t)}{dt} dt / \int_0^\infty \frac{dH(t)}{dt} dt \tag{7}$$
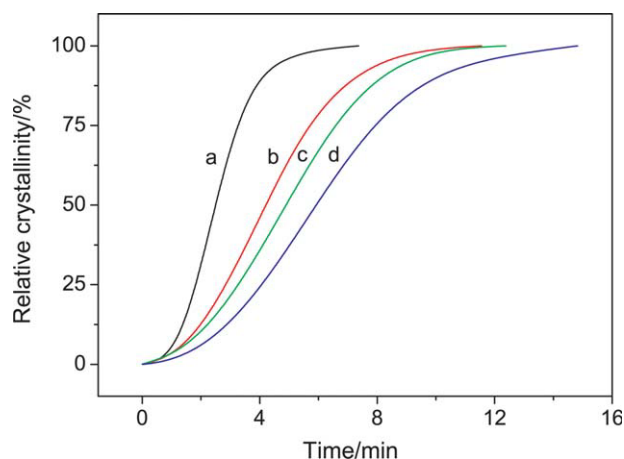
Figure 3 Development of relative crystallinity of PP/T-ZnOw composites with time during isothermal crystallization at 130 °C: (a) 100/0; (b) 100/1; (c) 100/3; (d) 100/5. [Color figure can be viewed in the online issue, which is available at wileyonlinelibrary.com.]

where $X(t)$ is the crystallinity of the sample at the crystallization time t, and $X(\infty)$ is the crystallinity of overall crystallization. Figure 3 shows the plot of X_c as a function of t. As shown in Figure 3, the shape of the curve of pure PP is sharp but it becomes smooth with increasing T-ZnOw content, which means it will take more time to achieve crystallization. To obtain n and K, the plot of $\log[-\ln(1 - X_c)$ versus $\log t$ was transformed, as shown in Figure 4.

In Figure 4, all curves showed good linear property, which means that the isothermal crystallization behaviors of PP/T-ZnOw can be analyzed effectively by the Avrami equation in this period. Based on n and K, the other crystallization kinetic parameters, i.e., t_{max}, $t_{1/2}$, and $G_{1/2}$ can be obtained accordingly. These data are summarized in Table II.
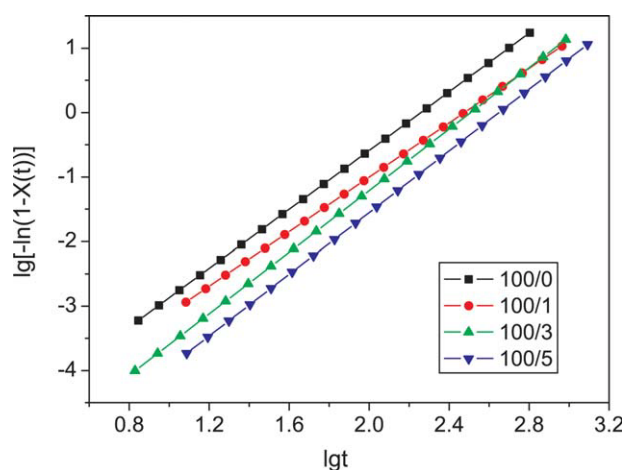
Figure 4 Avrami curves of the isothermal crystallization of PP/T-ZnOw composites at 130 °C. [Color figure can be viewed in the online issue, which is available at wileyonlinelibrary.com.]

TABLE II
**Kinetic Parameters of Isothermal Crystallization of PP/T-ZnOw Composites at 130 °C**

PP/T-ZnOw	n	$\log K$	$t_{1/2}$ (min)	t_{max} (min)	$G_{1/2}$ (min^{-1})
100/0	2.28	−5.15	2.58	2.35	0.38
100/1	2.11	−5.23	4.22	3.70	0.24
100/3	2.38	−5.98	4.65	4.32	0.21
100/5	2.39	−6.33	6.36	5.91	0.16

In general, n is nonintegral for most polymers, which indicates that the nucleating mechanism of the crystalline polymer is rather complicated and often includes both heterogeneous and homogeneous nucleation. Table II further shows that the n of PP/T-ZnOw composites, except that for the PP/T-ZnOw sample 100/1, are higher than that of pure PP. This proves that T-ZnOw does not have heterogeneous nucleation effects on the PP matrix, which is probably because the 3D structure of T-ZnOw is too complicated to induce PP molecular chains to assemble around it. It is found that the K and $G_{1/2}$ decreased, whereas $t_{1/2}$ and t_{max} increased, with increasing T-ZnOw content. These results indicate that filled T-ZnOw in PP retards crystal growth. Although the value of n in the sample PP/T-ZnOw (100/1) is slightly lower than that of pure PP, its t_{max} and $t_{1/2}$, are longer and its $G_{1/2}$ is lower than those of pure PP, indicating that it also retards the growth of the crystal. The reason for that is the 3D structure of T-ZnOw causes steric hindrance on PP crystallization. This can be confirmed by POM observations.

Crystallization morphology

Although the crystallization kinetics of the polymer can be investigated accurately by DSC measurement, polarized optical microscopy observation is more intuitive. Figure 5 shows the POM photographs of pure PP and PP/T-ZnOw composites crystallized at 130°C and 120°C, respectively. These two temperatures are used to observe the crystallization morphology for the comparison between a relatively high crystallization temperature and relatively low crystallization temperature. In the first line of Figure 5, the photographs show that the higher the T-ZnOw content, the fewer the number of crystal nuclei produced. This observation illustrates that the presence of T-ZnOw prevents the formation of PP crystal nuclei due to its complicated 3D structure; in the second line of Figure 5, the photographs show that the size of spherulitic crystals increases with increasing T-ZnOw content due to the reduction in the number of crystal nuclei. Thus, it can be conclude safely that T-ZnOw does not have heterogeneous nucleation effects on PP matrices.
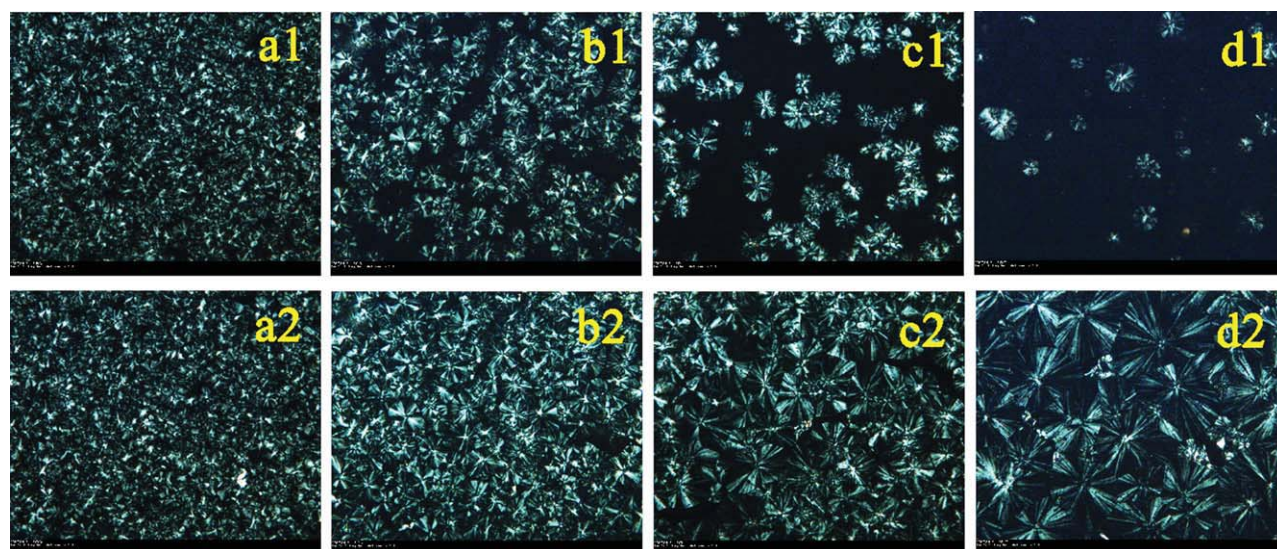
Figure 5 POM photographs of crystallized PP/T-ZnOw composites at 130 °C and 120 °C (200X): (a) 100/0; (b) 100/1; (c) 100/3; (d) 100/5; the first line: 130 °C; the second line: 120 °C. [Color figure can be viewed in the online issue, which is available at wileyonlinelibrary.com.
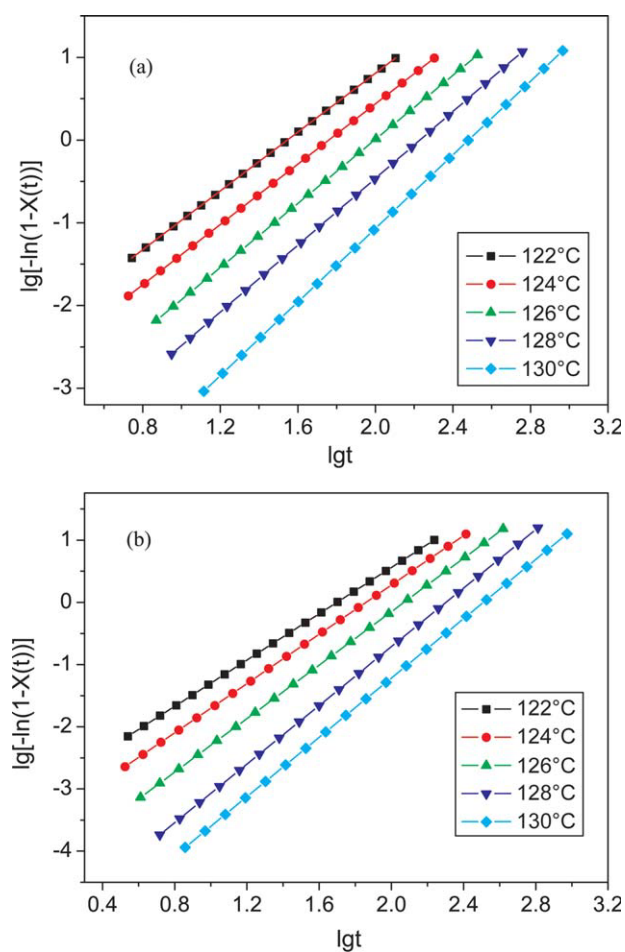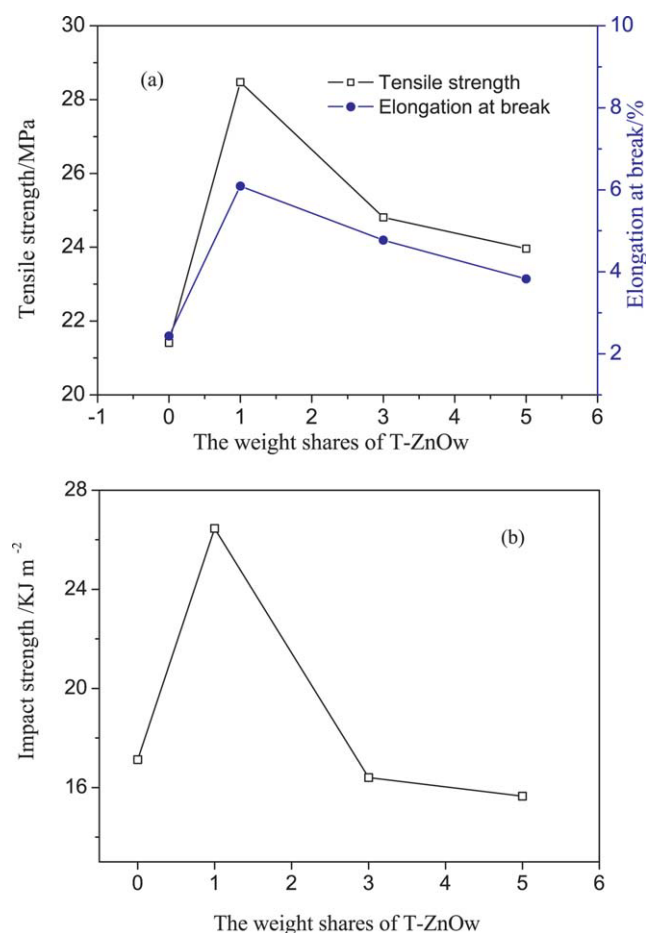

Figure 6 Avrami curves of isothermally crystallized PP/T-ZnOw composites at different temperatures: (a) 100/0; (b) 100/3. [Color figure can be viewed in the online issue, which is available at wileyonlinelibrary.com.]

Effect of crystallization temperature on isothermal crystallization behaviors

The crystallization temperature has a profound effect on crystallization behaviors. Because the crystallization is process of molecular chains reassembled around crystal nucleus, nucleation is regarded as a key factor and an essential prerequisite. If, on one hand, the temperature is too high, the crystal nucleus may become unstable or even fail to form due to the disruption of molecular motions. On the other hand, if the temperature is too low, the crystal growth stops because of the loss of molecular motion ability. A lower temperature is beneficial to the formation and stabilization of the crystal nucleus because there is more time to overcome the nucleation energy barriers. Higher temperatures result in the growth of the crystal due to the good activity of the molecular chains. Because the crystallization process includes two steps, i.e., nucleation and crystal

TABLE III
Kinetic Parameters of Isothermally Crystallized PP/T-ZnOw Composites at Different Temperatures

PP/T-ZnO$_w$	T_c (°C)	n	log$K$	$t_{1/2}$ (min)	t_{max} (min)	$G_{1/2}$ (min^{-1})
100/0	122	1.78	−2.75	0.46	0.37	2.10
	124	1.82	−3.21	0.79	0.62	1.26
	126	1.94	−3.87	1.36	1.13	0.73
	128	2.02	−4.50	2.35	2.01	0.43
	130	2.28	−5.15	2.58	2.35	0.39
100/3	122	1.86	−3.16	0.68	0.55	1.46
	124	1.98	−3.68	1.00	0.84	1.00
	126	2.14	−4.45	1.69	1.49	0.59
	128	2.36	−5.43	2.85	2.64	0.35
	130	2.38	−5.98	4.65	4.32	0.21

Figure 7 Mechanical performances of PP/T-ZnOw composites: (a) Tensile strength and elongation at break; (b)Impact strength. [Color figure can be viewed in the online issue, which is available at wileyonlinelibrary.com.]

growth, so the crystallization rate combines the contributions of both the nucleation rate and crystal growth rate.

Figure 6 shows the Avrami curves of pure PP and PP/T-ZnOw (100/3) at different isothermal crystallization temperatures. The corresponding crystallization kinetic parameters are summarized in Table III.

From Table III, it is found that the n increases with increasing isothermal crystallization temperature both for pure PP or PP/T-ZnOw composites but all of their values are no higher than 3. This illustrates that both heterogeneous and homogeneous nucleating mechanisms exist in these two systems. Although T-ZnOw has no heterogeneous nucleation effect on the PP matrix, the residual catalyst in the PP matrix often serves as a heterogeneous nuclear agent that can induce crystallization. Both $t_{1/2}$ and $t_{\max}$ increased, whereas the K and $G_{1/2}$ decreased significantly with increasing isothermal crystallization temperature. This was due to the reduction of the crystal nucleus at higher crystallization temperatures. The K and $G_{1/2}$ of PP/T-ZnOw

are minor compared to those of pure PP at the same crystallization temperature. The results indicate that filled T-ZnOw in PP retarded crystal growth.

Effect of T-ZnOw content on the mechanical performance of the PP/T-ZnOw composites

Figure 7 gives the mechanical performance of PP/T-ZnOw composites. As shown in Figure 7(a,b), the tensile and impact strength were synchronously enhanced when the weight ratio of PP/T-ZnOw was equal to 100/1; and it increased tensile strength by 33%, elongation at break by 151%, and impact strength by 55%, respectively. The fact illustrates that T-ZnOw has either a reinforcing or toughening effect on the PP matrix at lower weight ratios, although the T-ZnOw was not treated by any coupling agent. However, the reinforcing or toughening effect decreased when the weight ratio of the composite was over 100/1. The reason for that maybe: on one hand, T-ZnOw has a "nail" effect on the composite,[16] which carries and disperses stress to improve the mechanical performance of the composite; on the other hand, the presence of T-ZnOw increased the size of the spherulitic crystals, which caused the matrix to become brittle and led to the mechanical performance decreases. At very lower weight ratio, the "nail" effect is dominant; otherwise, the "size of the spherulitic crystals" effect is predominant.

CONCLUSIONS

In summary, the 3D structure of T-ZnOw causes steric hindrance on PP crystallization, which results in the absence of heterogeneous nucleation effects and retarded crystal growth of PP. The peak crystallization temperatures and melting temperatures deviated toward the direction of the lower temperatures when filled with T-ZnOw. The crystallization kinetic parameter K and $G_{1/2}$ decreased, whereas $t_{1/2}$ and $t_{\max}$ increased with increasing T-ZnOw content. T-ZnOw shows either a reinforcing or a toughening effect on the PP matrix at very lower weight ratio (100/1), but this effect declines with the increase in T-ZnOw content due to an increase in the size of the spherulitic crystal.

References

1. Mahfuz, H.; Adnan, A.; Rangari, V. K.; Jeelani, S.; Jang, B. Z. Compos A 2004, 35, 519.
2. Chen, J.; Chen, P.; Wu, L.; Zhang, J.; He, J. Polymer 2006, 47, 5402.
3. Tjong, S. C.; Meng, Y. Z. J Appl Polym Sci 1998, 70, 431.
4. Zhou, Z.; Peng, W.; Ke, S.; Deng, H. J Mater Process Technol 1999, 89–90, 415.
5. Chen, K.; Xiong, C.; Li, L.; Zhou, L.; Lei, Y.; Dong, L. Polym Compos 2009, 226.
6. Yshinaka, M.; Miyoshi, I; Asakura, E.; Shintaku, Y; Yoshida, H. EP0378995 (1993).

7. Iwanaga, H.; Fujii, M.; Takeuchi, S. J Cryst Growth 1998, 183, 190.
8. Zhou, Z.; Deng, H.; Yi, J.; Liu, S. Mater Res Bull 1999, 34, 1563.
9. Hu, G.; Ma, Y.; Wang, B. Mater Sci Eng A 2009, 504, 8.
10. Albano, C.; Papa, J.; Ichazo, M.; Gonzalez, J.; Ustariz, C. Compos Struct 2003, 62, 291.
11. Yuan, Q.; Awate, S.; Misra, R. D. K. Eur Polym J 2006, 42, 1994.
12. Wen, B.; Tang, W.; Tang, X. New Chem Mater 2009, 37, 87.
13. Huda, M. S.; Drzal, L. T.; Mohanty, A. K.; Misra, M. Compos B 2007, 38, 367.
14. Lin, Y.; Chen, H.; Chan, C.-M.; Wu, J. Macromolecules 2008, 41, 9204.
15. Ma, Y.-L.; Hua, G.-S.; Rena, X.-L.; Wang, B.-B. Mater Sci Eng A 2007, 460–461, 611.
16. Wang, Y.; Shi, J.; Han, L.; Xiang, F. Mater Sci Eng A 2009, 501, 220.